USING A WAVELET NETWORK TO CHARACTERIZE REAL ENVIRONMENTS FOR HAPTIC DISPLAY

Brian E. Miller
J. Edward Colgate

Department of Mechanical Engineering
Northwestern University
Evanston, IL 60208, USA
bemiller@nwu.edu colgate@nwu.edu

ABSTRACT

This paper will introduce a framework for characterizing real environments, using recorded force/displacement data, for use in haptic display. Steps in the framework include data acquisition, identification, model verification, and implementation. Identification and implementation will be developed in detail. After obtaining a conceptual understanding of the roles data acquisition and model verification play in the process, the methods used in this paper will be described. To meet the requirement for the identification stage, a proven technique in nonlinear system identification will be adopted. This technique, called wavelet network, will provide a tool that is capable of identifying environments with significant nonlinear features. A theoretical development along with experimental results will be presented using a spring attached to a wall. This environment exhibits a linear region with a single nonlinearity. The wavelet network was chosen because it was designed specifically for use with problems of high input dimension. Therefore, it is the expectation that the procedure will be useful in identifying environments of varying complexity. Currently, the technique can be used to identify static nonlinear environments. Work is being done to extend its capabilities to handle dynamic environments.

1 INTRODUCTION

Proposed haptic simulations have ranged from virtual walls [Colgate, et al. 1993, Salcudean and Vlaar 1994] and textures [Klatzky, et al. 1989, Minsky 1995], to complex static [Zilles and Salisbury 1995] and dynamic [Brown and Colgate 1997, Chang and Colgate 1997] environments and virtual prototyping [Hollerbach, et al. 1997]. Many of these methods use physics-based models in the development. The work here is directed toward providing a framework to characterize real environments for haptic simulation based on experimental force/displacement data. More specifically, the relationship between force and displacement is desired in order to characterize the impedance of the environment.

The motivation behind developing this framework is an attempt to address some issues concerned with rapid simulation development. This approach to the problem is in no way a replacement for current model-based techniques. Its purpose is to provide an additional tool for designers to use, one which may in some instances end up being the most effective.

The organization for the remainder of this section is as follows. First, the general framework for identification will be introduced. Following this, a discussion of related works will be presented that will highlight differences from the proposed method. The section will conclude with a detailed look at all the steps associated with the method presented here.

1.1 Framework

The goal of this paper is to introduce a framework for automating the task of environment design for haptic display. The necessary components are as follows:

- Obtain experimental Force/Displacement data
- Identify Environment
- Verify Model
- Implement Simulation

This paper will address in detail the issues concerning the second and forth steps in the above framework. The first step will be used to distinguish the proposed method from previous work.

1.2 Related Works

There have been a few reported works on developing at least some part of an environment using experimental data. All can be categorized using the above framework. A broader view of automated environment design can be found in [Dupont, et al. 1997, Schulteis, et al. 1996]. This section will briefly introduce each contribution and discuss the method of identification along with the procedure for data acquisition.

In [MacLean 1996] an identification technique, called the "Haptic Camera", was applied to a toggle switch to extract mass, damping, stiffness, and equilibrium point parameters to be used with an assumed model structure. The method worked by taking a signal, which is globally discontinuous and nonlinear, and dividing it into multiple zones. The number of zones, and thus the resolution, is controlled by a threshold parameter. Inside each zone the signal is assumed to be linear. Thus, the goal is to model the nonlinear phenomenon as a sequence of linear effects. Once this has been accomplished, the desired parameters can be extracted using well-developed linear identification techniques. To obtain the experimental data, the haptic device is used as an active probe under computer control. To extract the desired parameters, an appropriate trajectory is commanded and the resulting forces recorded. The technique is automated in the sense that it requires no designer interaction until the simulation is ready for implementation.

Another identification technique was applied to the area of minimally invasive surgery to model the properties of human tissue [Scilingo, et al. 1997]. A laparoscoptic tool was fitted with sensors to record contact force and tissue deformation. To collect the data, a surgeon uses the tool that will record the forces imposed on the forceps jaws and the deformation of the tissue being manipulated. This data was used to extract parameters associated with inertial, stiffness and damping characteristics. The parameters were found by obtaining a least square solution to an over-determined system of equations.

Along with an assumed model structure, nonlinear equations were defined based on knowledge of tissue characteristics.

The above contributions provide examples of two different methods for data acquisition. The "Haptic Camera" used the haptic display as an active probe and commanded it to interact with the environment. The minimally invasive surgery example monitored force/displacement through human interaction with the environment.

Both of the above techniques focus on extracting parameters for an assumed model that governs the behavior of the environment. This is the main point that sets the proposed work apart from previous work. This paper focuses on creating the model for the target environment, which requires no a priori knowledge about the *shape* of the impedance characteristic being identified.

1.3 Detailed Framework

This section will discuss in detail the experimental setup for the technique proposed in this paper. The first three steps in the framework will be described.

1.3.1 Data Acquisition

A one-degree of freedom (DOF) haptic display will be used as an inspection probe through human exploration to collect force/displacement data. The components of the device are a motor with collocated encoder sensing, a physical damper, and handle with a .15 meter moment arm that serves as the interface to the human. The haptic display is an impedance device (senses position, outputs force), however, for the purpose of identification a force transducer is placed collinear with the shaft of the motor. Neglecting any dynamics between the transducer and motor, the measured torque corresponds to the necessary motor torque to describe the target environment. The force transducer is a 6-axis force/torque sensor from Assurance Technologies Inc. model 15/50. Since the haptic display is only one DOF, only the z-axis torque measurement will be recorded, which has the capability of measuring between $\pm$ 5 N-m. The sampling frequency for all data acquisition, as well as implementation, will be 1 kHZ.

1.3.2 Identification Technique

The procedure used is a proven method for nonlinear system identification. The identification tool is called a wavelet network [Zhang and Benveniste 1992]. It has been shown that wavelet networks exhibit the same approximation capabilities as traditional neural networks, however they posses better initialization characteristics due to the strong influence of wavelet theory in constructing the network [Zhang and Benveniste 1992]. The wavelet network will perform a nonlinear nonparametric regression estimation on a given set of data. This will allow the impedance characteristic of an environment to be identified, resulting in a model. A MATLAB® toolbox obtained from [Zhang 1993], described in [Zhang 1997], will be used to obtain the model for the environment.

1.3.3 Model Verification

Once the model has been identified its quality needs to be verified. As a first step, the output of the environment model can be compared to the measured data. This will assure that a well-behaved model has been produced. This is the extent to which this paper will address the issue.

Producing a well-behaved model is only one step in assessing the success of the identification procedure. A more rigorous analysis would be to perform psychophysical tests to determine if the appropriate perceptual features of the environment were captured.

1.4 Remainder of the Paper

Before proceeding with implementation issues, it seems appropriate to digress briefly and present an introduction to wavelets.

Section 2 will introduce the theory underlying the wavelet network. Section 3 will take a detailed look at the wavelet network and its structure. Section 4 will introduce a development leading to implementation. Section 5 will provide experimental results based on the development in Section 4. The final section will present conclusions and discuss future work.

2 WAVELETS

Wavelets are a powerful tool for function analysis and synthesis. In this section the concept of wavelets will be presented through a simple example. To begin the discussion, a brief introduction to the continuous wavelet transform and inverse wavelet transform will be given. Following this, a comparison with Fourier analysis will be presented to highlight the strengths of wavelet theory. The environments being considered will result in functions dependent on state (position) as opposed to time. Therefore, the domains of interest will be space-frequency as opposed to time-frequency. This section concludes with a discussion on discrete implementations of the inverse wavelet transform, which is the form used in the wavelet network.

2.1 Continuous Wavelet Transform

The continuous wavelet transform (CWT) can be expressed as follows:

$$w_i(\alpha,\beta) = \int f(x)\psi(\alpha x-\beta)dx \qquad (1)$$

The parameter α controls the width (dilation) of the wavelet, while β controls the position (translation). The variable ψ is a family of functions based on a single analyzing wavelet, along with its translated and dilated versions. The result of this transform is a set of wavelet coefficients, ranging over different widths of wavelets, called levels. The translation parameter is adjusted according to the dilation parameter to ensure that the entire operating range is covered. As an example of what a family of analyzing wavelets would look like, consider the Mexican hat (second derivative of the Gaussian) wavelet in Figure 1.

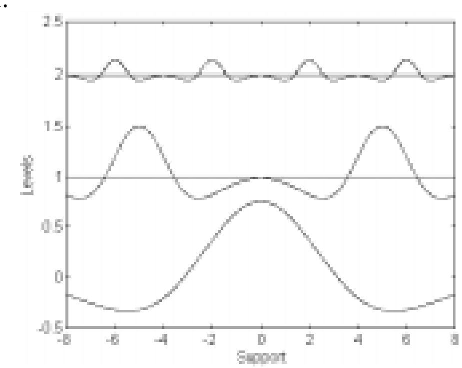

Figure 1: A conceptual view of how the wavelet transform works using a Mexican hat wavelet.

The wavelet transform analyzes a function at different *wavelet levels.* A *wavelet level* is defined as a set of translated wavelet with constant dilation. Wavelets have been compared to microscopes [Rioul and

Vetterli 1991] with the ability to zoom in on short lived high frequency features. This fact can be noted by observing that as the wavelet becomes more contracted, it approaches a discontinuity. Using more levels in the analysis results in the ability to extract more detailed (high frequency) features.

Of greater interest to this work is how to use wavelet theory to reconstruct functions. This is achieved by applying the inverse wavelet transform:

$$f(x) = \iint w_i(\alpha,\beta)\psi(\alpha x - \beta)d\alpha d\beta \quad (2)$$

which states that a function can be reconstructed by summing over the entire range of translated and dilated wavelets.

2.2 Wavelet and Fourier Analysis

Fourier analysis shows that any periodic function can be represented by the sum of sines and cosines. Similarly, wavelet theory shows that an arbitrary function can be represented by the sum of wavelets. Applying the Fourier transform and the wavelet transform to the force history curve shown in Figure 2 (a), the following points regarding wavelet theory will be highlighted:

- Wavelets are capable of representing functions that are choppy, discontinuous, and potentially non-periodic.
- The wavelet transform represents the function in both space and scale (frequency), while the Fourier transform addresses frequency alone.

Figure 2 (b) and (c) show an example of the wavelet transform and Fourier transform respectively.

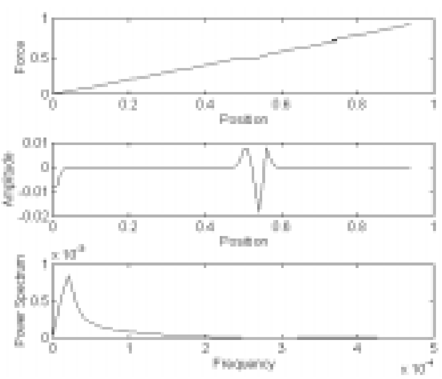

Figure 2: (a) Force-History, (b) Wavelet analysis (most detailed level), (c) Fourier analysis.

The wavelet analysis was conducted using the continuous wavelet transform as discussed in Section 2.1. A plot of the most detailed *wavelet level* in the CWT is shown in Figure 2 (b). The amplitude axis in this plot corresponds to the magnitude of the wavelet coefficients, which displays how well the wavelets 'match' the signal [Lewalle 1995]. One can see that not only has frequency information been identified, but the location has been pinpointed as well. The relationship between the width (scale) of the wavelet and the frequency it represents is developed in [Lewalle 1995]. The Fourier analysis, represented in the form of a power spectrum, has extracted the frequency content of the force-history, however the information relating to location has been lost.

An advance in Fourier analysis provides a method to represent a function in both space and frequency. The concept is referred to as the short time Fourier transform (STFT). The basic approach is to fix a window size of constant length, and change the frequency within the window using a finite section of a sine or cosine function. Once the window size has been defined it remains constant throughout the entire space-frequency plane. Although the approach is sensible, it suffers from the issue of defining window size. If the window is large then low frequency content is captured but it becomes difficult to pinpoint the location of high-frequency *features*. If the window size is small then high frequency *features* are captured with good accuracy, however the low-frequency content is missed. Based on the above notion it would be nice if both large and small windows could be used. This is precisely what wavelet theory provides. Wavelets automatically adjust the size of the window, through the dilation parameter, to compensate for high and low frequency content.

The above comparison was a brief introduction into the differences between Fourier and wavelet analysis. The intent was to introduce some characteristics inherent to wavelet analysis that make it a powerful tool when applied to nonlinear functions. For a full and detailed comparison between Fourier and wavelet theory, the reader is referred to [Daubechies 1990].

2.3 Discretization Methods

Since the functions of interest to this work will always consist of data points sampled at a constant time step, it is appropriate to obtain a discretized version of the inverse wavelet transform (2). There are various methods for obtaining a discretized version of (2). The general structure for the inverse discrete wavelet transform is as follows:

$$f(x) = \sum_i w_i \psi(\alpha_i x - \beta_i) \quad (3)$$

For stable reconstruction of the function, the above form must meet certain criteria. One common way is to construct a family of wavelets that constitute an orthonormal basis. Another method is to create a family of wavelets that constitute a frame.

2.4 Bases vs. Frames

An orthonormal basis is a set of wavelet functions that are linearly independent, which can be used to represent any function within a functional space. Normally a regularly spaced grid of points is used with constants, α_o and β_o defining the step sizes for the translation and dilation parameters, such that the wavelets are orthonormal. Orthonormal bases have the desired property that very efficient algorithms have been developed for use with them. As a result, many practical applications such as signal and image processing have utilized this form.

To approximate nonlinear functions of high input dimension (p), multidimensional wavelets are required. For computational reasons it is desirable to build frames from single-scaling wavelets (wavelets using a single dilation parameter in all dimensions). It has been shown in [Kugarajah and Zhang 1995], as the dimension of the wavelets increase, particularly when p>3, it becomes difficult to implement multidimensional wavelets using single-scaling orthonormal bases. Further development in [Kugarajah and Zhang 1995] shows that using wavelet frames provides a convenient method for constructing multidimensional wavelets. The concept of a frame will be introduced through an example. For a complete discussion on frames the interested reader is referred to [Daubechies 1992].

The following simple example, adapted from [Daubechies 1990, Strang and Nguyen 1996], will help clarify the concept of a frame.

Consider a set of vectors in $\Re^2$:

$$r_1 = (0,1); r_2 = \left(\frac{\sqrt{3}}{2}, \frac{1}{2}\right); r_3 = \left(\frac{\sqrt{3}}{2}, -\frac{1}{2}\right)$$

One can see that these vectors do not form an orthonormal basis because they are not independent, however they span $\Re^2$. Therefore, any vector **v** in $\Re^2$ can be expressed as $\mathbf{v} = \sum_i b_i r_i$. Inserting the vectors as rows into a matrix **T**, forms what is referred to as the *frame operator*:

$$\mathbf{T} = \begin{bmatrix} 0 & 1 \\ \frac{\sqrt{3}}{2} & \frac{1}{2} \\ \frac{\sqrt{3}}{2} & -\frac{1}{2} \end{bmatrix}$$

To retrieve the vector **v** the inverse of the frame operator is required. Since **T** is not a square matrix, the pseudo-inverse will be computed. Obtaining a new operator, $\mathbf{T}^{\mathbf{T}}\mathbf{T}$, will provide an invertible matrix that has the same rank as **T**:

$$\mathbf{T}^{\mathbf{T}}\mathbf{T} = \begin{bmatrix} \frac{3}{2} & 0 \\ 0 & \frac{3}{2} \end{bmatrix}$$

The eigenvalues of the above operator are defined to be the frame bounds. Since they are equal, the vectors form a *tight* frame. There are a number of ways to obtain the inverse, however [Strang and Nguyen 1996] shows that the inverse $\mathbf{T}^{+}=(\mathbf{T}^{\mathbf{T}}\mathbf{T})^{-1}\mathbf{T}^{\mathbf{T}}$ works the best.

$$\mathbf{T}^{+} = \begin{bmatrix} 0 & \frac{\sqrt{3}}{3} & \frac{\sqrt{3}}{3} \\ \frac{2}{3} & \frac{1}{3} & -\frac{1}{3} \end{bmatrix}$$

The column vectors of $\mathbf{T}^{+}$ are referred to as the dual frames. Consider a vector $\mathbf{v} = (1\ 1)^{\mathbf{T}}$ in $\Re^2$. Representing **v** in terms of the basis vectors :

$$b_1 = \langle r_1, \mathbf{v} \rangle = 1$$

$$b_2 = \langle r_2, \mathbf{v} \rangle = \frac{\sqrt{3}}{2} + \frac{1}{2}$$

$$b_3 = \langle r_3, \mathbf{v} \rangle = \frac{\sqrt{3}}{2} - \frac{1}{2}$$

To retrieve the vector **v**:

$$\mathbf{v} = \sum_i b_i r_i = \begin{bmatrix} 0 & \frac{\sqrt{3}}{3} & \frac{\sqrt{3}}{3} \\ \frac{2}{3} & \frac{1}{3} & -\frac{1}{3} \end{bmatrix} \begin{bmatrix} 1 \\ \frac{\sqrt{3}}{2} + \frac{1}{2} \\ \frac{\sqrt{3}}{2} - \frac{1}{2} \end{bmatrix} = \begin{bmatrix} 1 \\ 1 \end{bmatrix}$$

The fact that the frame bounds are finite means that any vector in $\Re^2$ can be stably recovered by $\mathbf{v} = \sum_i b_i v_i$.

The above development extends to families of functions. The conditions to construct a wavelet frame in one-dimension were developed in [Daubechies 1992]. These results were extended in [Kugarajah and Zhang 1995] to allow the construction of multidimensional wavelet frames that are useful for function identification. Wavelets families that constitute a frame are used in the wavelet network [Zhang 1997].

3 ENVIRONMENT MODEL

3.1 Nonparametric Regression Estimation

The wavelet network performs a nonlinear nonparametric regression estimation on a given set of data.

The following model will be assumed:

$$y = f(x) + e$$

Where the variable y represents the output, $f(x)$ is some unknown nonlinear function with respect to the input ($\boldsymbol{x}$). The variable e represents noise, which is independent of $\boldsymbol{x}$. A sequence of data is collected from the environment, $X \in \Re^d, Y \in \Re$:

$$X = \{x_1, \ldots, x_n\}, Y = \{y_1, \ldots, y_n\}$$

The task will be to find some nonlinear nonparametric estimate, $\hat{f}$, that closely approximates f according to some functional measure. For this particular implementation the measure of choice is the mean squared error (MSE).

$$MSE = \frac{1}{N} \sum_{k=1}^{N} \left(\hat{f}(x_k) - y_k \right)^2$$

3.2 Network Structure

This section will provide a brief overview of the wavelet network. A more detailed presentation can be found in [Zhang 1997].

The wavelet network takes the following form:

$$f(x) = \sum_{i=1}^{N} w_i \psi\left(\alpha_i * (x - \beta_i)\right)$$

Where $w_i \in \Re, \alpha_i \in \Re^d, \beta_i \in \Re^d$, are the network parameters, and correspond to the wavelet coefficient, dilation parameter and, and translation parameter respectively. The variable N is the number of wavelets, and "$*$" denotes component-wise multiplication of vectors. The role of the wavelet network is to construct a discretized wavelet family by adapting the network parameters to the force/displacement data. To obtain the best set of wavelets for use in the network the following steps are taken:

- An initial set of wavelets (S) is defined based on the available data. This set is obtained by eliminating any wavelet from a truncated (finite) frame whose supports do not contain any input data.
- Viewing the wavelets as regression candidates, a regressor selection algorithm is applied that will identify the members of the set S which contribute most to identifying f. Once this has been completed an initial approximation to the model can be obtained by solving a least-squares problem to obtain the w_i's. The quality of the model is evaluated by analyzing a fresh data set and calculating the MSE. If the results are favorable, then the model is complete, otherwise the next step should be taken.
- The first two steps have provided an excellent initialization for the network. To further enhance the quality of the model, a backpropagation algorithm can be applied to adjust the network parameters. Due to the good initialization properties, the more efficient quasi-Newton procedure can be used [Luenberger 1996].

3.3 Final Model

The identification process will be applied to a class of environments that typically exhibit linear regions along with the nonlinearities. In order to produce a result that captures both of these aspects the final model takes the form:

$$f(x)=\sum_{i=1}^{N} w_i \psi\left(\alpha_i*\left(x-\beta_i\right)\right)+c^T x+b \qquad (4)$$

The parameters $c \in \Re^d, b \in \Re$ are the linear coefficients and bias term respectively. Recall that N is the number of wavelets in the network.

This paper will use the Mexican hat wavelet. The wavelet family, which constitutes a frame, consists of the analyzing wavelet located at the origin along with its translated and dilated versions:

$$f(x)=\sum_{i=1}^{N} w_i\left(\left(\alpha_i\left(x-\beta_i\right)\right)^2-1\right)e^{-.5\left(\alpha_i\left(x-\beta_i\right)\right)^2}+c\cdot x+b \qquad (5)$$

The identified environment model will be in the form of (5). Once α and β are obtained from the initialization procedure they are used in computing a least squares solution for *w*, *c*, and *b*.

$$\begin{bmatrix} \left(\left(\alpha_1\left(x_1-\beta_1\right)\right)^2-1\right)e^{-.5\left(\alpha_1\left(x_1-\beta_1\right)^2\right)} & \cdots & \left(\left(\alpha_N\left(x_1-\beta_N\right)\right)^2-1\right)e^{-.5\left(\alpha_N\left(x_1-\beta_N\right)^2\right)} & x_1 & 1 \\ \vdots & \vdots & \vdots & \vdots & \vdots \\ \left(\left(\alpha_1\left(x_n-\beta_1\right)\right)^2-1\right)e^{-.5\left(\alpha_1\left(x_n-\beta_1\right)^2\right)} & \cdots & \left(\left(\alpha_N\left(x_n-\beta_N\right)\right)^2-1\right)e^{-.5\left(\alpha_N\left(x_n-\beta_N\right)^2\right)} & x_n & 1 \end{bmatrix} \begin{bmatrix} w_1 \\ \vdots \\ w_N \\ c \\ b \end{bmatrix} = \begin{bmatrix} y_1 \\ \vdots \\ \vdots \\ \vdots \\ y_n \end{bmatrix}$$

The variable *n* represents the number of force/displacement pairs recorded.

4 CONTROL STRUCTURE

The final step in designing a simulation for haptic display is incorporating it into the control structure. A block diagram of the one DOF haptic display is shown in Figure 6.

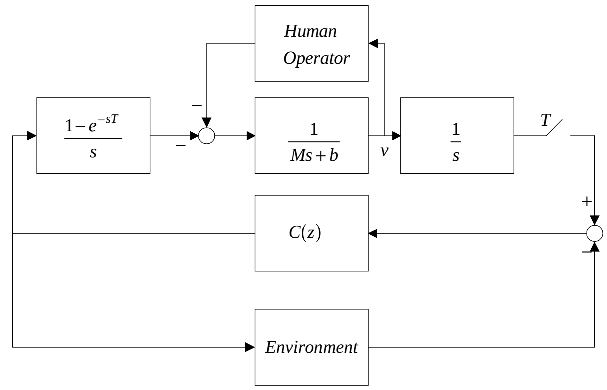

Figure 6: Haptic Control Structure.

The motivation behind the above control structure is that it isolates the design of the environment from the issues of the data sampled system through the use of the virtual coupling [Colgate, et al. 1995]. The virtual coupling is denoted by C(z) in the above block diagram.

4.1 The Virtual Coupling

Figure 7 shows a one-dimensional interpretation of a spring/damper virtual coupling. This interpretation of the virtual coupling can be used with admittance modeled environments displayed on an impedance haptic display.

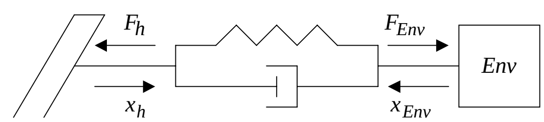

Figure 7: Conceptual View of Virtual Coupling.

In general, unless the impedance is monotonically increasing, a mapping from force to position will not be unique. However, a unique mapping from position to force will always exist. To accommodate the environment causality a new interpretation of the virtual coupling is necessary. One possible choice is a mass-spring-damper configuration:

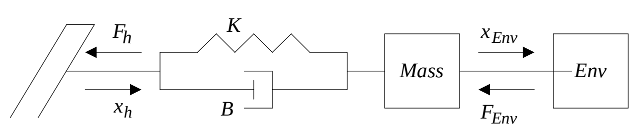

Figure 8: Mass, Spring, Damper Virtual Coupling.

A concern regarding the above configuration is that the mass will add some unwanted dynamics to the environment behavior. Furthermore, the choice for K and B follows from the fact that any haptic display can exhibit a finite range of impedances referred to as the Z-width of the device [Colgate and Brown 1994]. The stiffness and damping parameters are chosen based on the hardware, and sampling time, to ensure that the device does not attempt to render an impedance above its capabilities. The choice for the mass value is not quite as clear and could adversely affect the identified environment. It would be convenient for both the design of the virtual coupling and the identification of the environment to group the mass with the environment. This eliminates it from the virtual coupling, and allows the identification algorithm to incorporate it in the environment model. In the development that follows, a new environment structure will be defined that incorporates the mass.

4.2 Environment Structure

Consider the bond graph for an impedance haptic display and an impedance modeled environment.

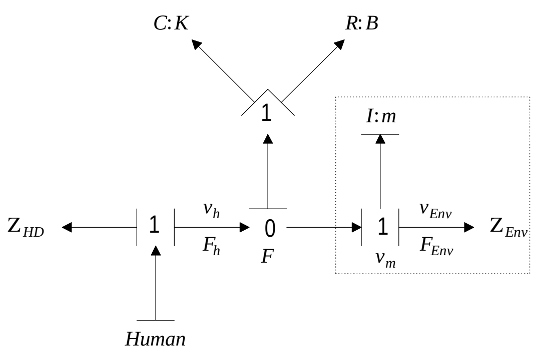

Figure 9: Bond Graph of Impedance Haptic Display and Impedance Modeled Environment

The new environment structure corresponds to the branch of the bond graph enclosed by the dotted box in Figure 9. This leaves the parallel spring/damper as the connection point between the environment and haptic display.

In reduced block diagram form, the environment structure becomes:

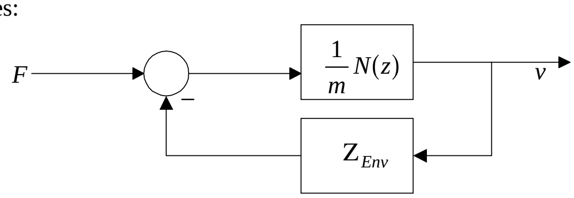

Figure 10: General Environment Model Structure

N(z) is a linear shift invariant transfer function. Physical insight suggests it should act as an integrator.

Based on the general environment model structure, methods for identification and implementation of static environments can be defined, and are shown below in block diagram form.

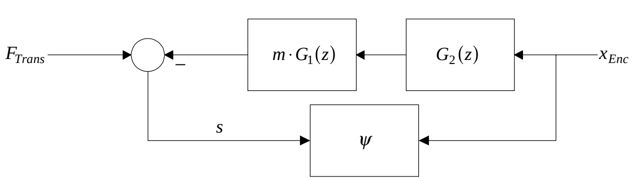

Figure 11: Identification

F_{Tran} and x_{Enc} represent the recorded data from the force transducer and encoder.

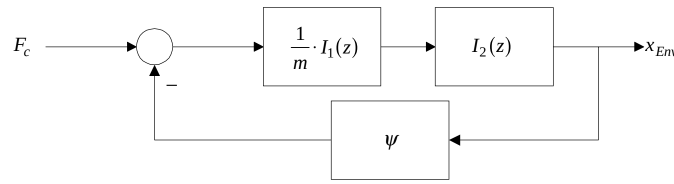

Figure 12: Implementation

F_c represents the force from the virtual coupling and x_{Env} is the updated environment position.

$G_1(z), G_2(z), I_1(z)$ and $I_2(z)$ are linear shift invariant transfer functions that need to be defined. An obvious choice would be to choose suitable integrators for I_1 and I_2 and then use the inverse for G_1 and G_2. An alternative choice, used in this paper, is to design G_1 and G_2 to approximate differentiation but roll off at high frequency to help suppress noise. To keep the implementation as close as possible to the identified model, G_1 and G_2 are designed so that they match I_1^{-1} and I_2^{-1} exactly up to a certain frequency.

4.3 Implicit vs. Explicit

This section will investigate particular choices for the linear sub-blocks in Figures 11 and 12.

The first set of choices will result in a nonlinear implicit equation to solve for position.

Choosing,

$$I_1(z) = I_2(z) = \frac{Tz}{z-1}$$

and designing

$$G_1(z) = G_2(z) = \frac{14.8379 \cdot \left(z^2 - 1\right)}{\left(z^2 - 1.6556z + .68518\right)}$$

,which matches I_1^{-1} and I_2^{-1} almost exactly up to 100 rad/sec, results in the following implicit nonlinear equation.

$$x_k + T^2 \psi\left(x_k\right) = 2x_{k-1} - x_{k-2} + T^2 F_k$$

Solving for the desired output, s, requires future values of the input, however since the identification is done off-line the algorithm has access to this data. The trouble occurs during implementation. The implicit equation must be solved through iteration, which makes it undesirable for real time applications. In some cases it is possible to implement an efficient algorithm that is capable of producing the solution in the allotted time, however as the environments become more complex it will soon become infeasible.

To obtain an explicit equation for position, a delayed integrator must be used for I_1. Choosing

$$I_1(z) = \frac{T}{z-1}$$

requires a redesign of G_1:

$$G_1(z) = \frac{31\cdot(z-1)}{\left(z^2 - 1.6556z + .68518\right)}$$

so that $G_1$and I_1^{-1} will match to approximately 100 rad/sec. I_2 and G_2 will remain the same. The expression for position becomes:

$$x_k = 2x_{k-1} - x_{k-2} + T^2\left(F_{k-1} - \psi\left(x_{k-1}\right)\right)$$

Applying this development to a real environment resulted in a position response that was oscillatory.

To determine if the oscillations were produced by the wavelets or the linear part of the system, Equation 5 was linearized about zero and the root locus was drawn with respect to the gain in the feedback loop (which is a function of wavelet parameters). The root locus revealed that the delay forced the roots of the linearized model to the boundary of the unit circle. To compensate for the destabilizing effect of the delay, a linear damping term is added as an inner feedback loop.

Using a delayed integrator requires a modification to the identification and implementation structures.

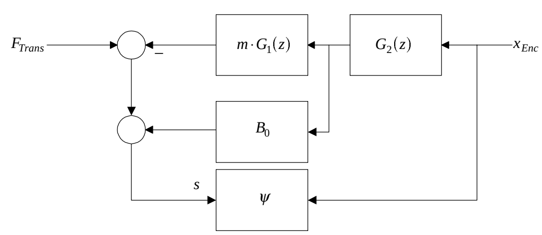

Figure 13: Modified Identification Structure

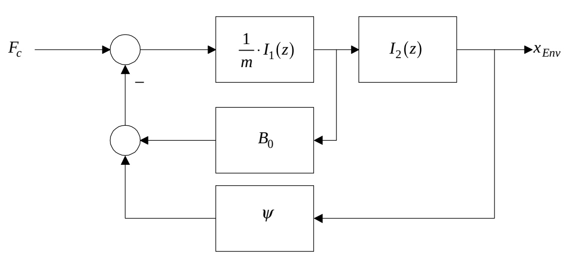

Figure 14: Modified Implementation Structure

5 EXPERIMENTAL RESULTS

Experimental results will be presented using the modified structures in Figures 13 and 14. Using the experimental setup described in Section 1.3.1, force and displacement data will be recorded. Using the recorded data and solving for the desired output, *s*, a Matlab™ toolbox obtained from [Zhang 1993][1], will define the nonlinear block, ψ, based on a wavelet network. For the environments considered thus far, the amount of time from data collection to final model was approximately four to five minutes.

A spring rigidly fixed in space will be used for the real environment. The force history curve of this environment is fairly linear until the point where the coils are contracted together which results in a large transition in the impedance characteristic approaching the behavior of a wall. This environment is an example of the special case where the impedance characteristic is monotonically increasing, however the next section will show that the environment structure can still be used to characterize the impedance.

5.1 Spring Attached to a "Wall"

The parameters that need to be chosen during the identification stage are the mass value and linear damping term (B_o). Recall that the mass was necessary to reverse causality of the environment so the spring/damper virtual coupling can be used. Currently, the wavelet network identifies the entire environment, therefore the mass can be viewed as an added inertia. This provides motivation to make it as small as possible. The damping term, B_o, needs to be chosen such that it adequately compensates for the delay. This can be accomplished by linearizing the model about an equilibrium point (zero force, zero position) and plotting the root locus with respect to the feedback term. Adjusting the damping will move the branches to more desirable locations. Choosing a mass value of m=.001 kg and a damping value of B_o=.5 N-m-s the nonlinear block was identified using the structure in Figure 13. Using the implementation structure in Figure 14, the environment was simulated using recorded torque data. The actual impedance characteristic, obtained through force transducer and encoder measurements, is compared to the identified impedance characteristic.

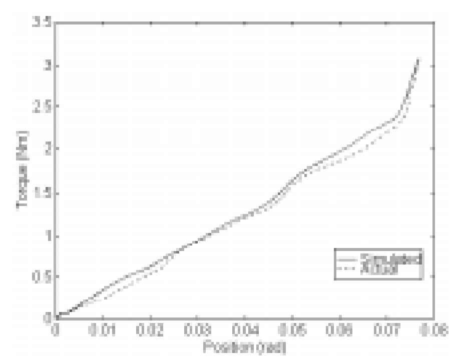

Figure 15: Actual Impedance Characteristic (dotted line) compared to Identified Impedance Characteristic (solid line).

Although the above environment was very simple, it allowed for a detailed analysis to determine how to implement a successful identification procedure.

6 DISCUSSION AND FUTURE WORK

One concern regarding the above procedure is that the mass in the forward path is viewed as an unwanted inertia. A more appropriate way to conduct the identification would be to reformulate the

[1] The code that solves for the linear terms was slightly modified

procedure so that the mass value is determined based on the experimental data. Future work will make this adjustment.

Another target of future work will be to conduct psychophysics experiments to provide a more accurate measure of the identification procedure's success. Application to dynamic systems will also be a target of future research.

REFERENCES

[1] J. M. Brown and J. E. Colgate, "Passive Implementation of Multibody Simulations for Haptic Display," presented at International Mechanical Engineering Congress and Exhibition, Dallas, TX, 1997.

[2] B. Chang and J. E. Colgate, "Real-time Impulse-based Simulation of Rigid Body Systems for Haptic Display," presented at International Mechanical Engineering Congress and Exhibition, AMSE, Dallas, TX, 1997.

[3] J. E. Colgate and J. M. Brown, "Factors Affecting the Z-width of a Haptic Display," presented at International Conference on Robotics and Automation, San Diego, CA, 1994.

[4] J. E. Colgate, P. E. Grafing, M. C. Stanley, and G. Schenkel, "Implementation of Stiff Virtual Walls in Force-Reflecting Interfaces," presented at IEEE Virtual Reality Annual International Symposium, Seattle, WA, 1993.

[5] J. E. Colgate, M. C. Stanley, and J. M. Brown, "Issues in the Haptic Display of Tool Use," presented at IEEE/RSJ International Conference on Intelligent Robots and Systems, Pittsburgh, 1995.

[6] I. Daubechies, "The Wavelet Transform, Time-Frequency Localization and Signal Analysis," *IEEE Transactions on Information Theory*, vol. 36-5, pp. 961-1005, 1990.

[7] I. Daubechies, *Ten Lectures on Wavelets, CBNS-MSF regional series in applied mathematics*. Philadelphia: SIAM, 1992.

[8] P. E. Dupont, T. M. Schulteis, and R. D. Howe, "Experimental Identification of Kinematic Constraints," presented at International Conference on Robotics and Automation, Albuquerque, New Mexico, 1997.

[9] Hollerbach, Cohen, Thompson, Freier, Johnson, Nahvi, Nelson, Thompson, and Jacobsen, "Haptic Interfacing for Virtual Prototyping of Mechanical CAD Designs," presented at ASME Design for Manufacturing Symposium, Sacramento, CA, 1997.

[10] R. Klatzky, S. Lederman, and C. Reed, "Haptic Integration of Object Properties: Texture, Hardness, and Planar Contour," *J. of Exp. Psychology: Human Perception and Performance*, vol. 15, pp. 45-57, 1989.

[11] T. Kugarajah and Q. Zhang, "Multidimensional Wavelet Frames," *IEEE Transactions on Neural Networks*, vol. 6-6, pp. 1552-1556, 1995.

[12] J. Lewalle, "Wavelets Tutorial," , 1995.

[13] D. G. Luenberger, *Linear and Nonlinear Programming*. Reading, MA, 1996.

[14] K. MacLean, "The "Haptic Camera": A Technique for Characterizing and Playing Back Haptic Properties of Real Environments," presented at Proceeding ASME Dynamics Systems and Control Division, 1996.

[15] M. D. R. Minsky, "Computational Haptics: The Sandpaper System for Synthesizing Texture for a Force-Feedback Display," : Media Lab, MIT, 1995.

[16] O. Rioul and M. Vetterli, "Wavelets and Signal Processing," in *IEEE SP Magazine*, 1991, pp. 14-35.

[17] S. E. Salcudean and T. D. Vlaar, "On the Emulation of Stiff Walls and Static Friction with a Magnetically Levitated Input/Output Device," presented at International Mechanical Engineering Exposition and Congress, Chicago, IL, 1994.

[18] T. M. Schulteis, P. E. Dupont, P. A. Millman, and R. D. Howe, "Automatic Identification of Remote Environments," presented at Proceedings of the ASME Dynamics Systems and Control Division, Atlanta, 1996.

[19] E. Scilingo, D. De Rossi, A. Bicchi, and P. Iacconi, "Haptic display for replication fo rheological behaviour of surgical tissues: modelling, control, and experiments," presented at International Mechanical Engineering Congress and Exhibition, Dallas, TX, 1997.

[20] G. Strang and T. Nguyen, *Wavelets and Filter Banks*, 1996.

[21] Q. Zhang, "Wavenet," , Anonymous FTP: ftp.irisa.fr:/local/wavenet ed, 1993.

[22] Q. Zhang, "Using Wavelet Network in Nonparametric Estimation," *IEEE Transaction on Neural Networks*, vol. 8-2, pp. 227-236, 1997.

[23] Q. Zhang and A. Benveniste, "Wavelet Networks," *IEEE Transactions on Neural Networks*, vol. 3-6, pp. 889-898, 1992.

[24] C. Zilles and K. Salisbury, "A Constraint-Based God Object Method for Haptic Display," presented at International Conference on Intelligent Robots and Systems, Pittsburgh, 1995.